

## Scaling theory for the optical properties of semicontinuous metal films

Y. Yagil, M. Yosefin,\* D. J. Bergman, and G. Deutscher

*Department of Physics and Astronomy, Raymond and Beverly Sackler Faculty of Exact Sciences,  
Tel Aviv University, 69978 Tel Aviv, Israel*

P. Gadenne

*Laboratoire d'Optique des Solides, Université Pierre et Marie Curie, 4 Place Jussieu,  
75230 Paris CEDEX 05, France*

(Received 6 September 1990; revised manuscript received 2 January 1991)

The optical properties of thin semicontinuous metal films are calculated within the framework of the scaling theory of percolation. The effective ac conductivity is calculated over a length scale determined by the optical frequency. The relevant length scale depends on the frequency through the anomalous diffusion relation. At finite frequencies the ac conductivity fluctuates over the surface of the film, resulting in fluctuations of the local optical response. These fluctuations are described by a broad bimodal distribution. The optical response of the whole film is then calculated by averaging the local contributions, using the above distribution function. We find that the inter-cluster capacitance is essential in understanding the optical response of a percolating film. Numerical calculations based on this model show excellent agreement with experimental data over the entire range of surface coverages.

### I. INTRODUCTION

The optical properties of metal-insulator mixtures have been much investigated, both experimentally and theoretically. Semicontinuous metal films [two-dimensional (2D) material] are normally prepared by thermal evaporation or sputtering of the metal on an insulating substrate, and cermets (3D material) by coevaporation or cosputtering of both metal and insulator.

In the growing process, small metallic grains, with typical size of 5–30 nm (controlled by the preparation conditions) are formed on the substrate. For semicontinuous metal films, as the film grows further, the filling factor increases and coalescence occurs, so that irregularly shaped clusters are formed. As more metal is evaporated, these clusters grow further and form fractal structures, the size of which diverges as the film approaches the percolation threshold. At that point, a spanning or percolating cluster of metal is formed so that there now exist continuous conducting paths from one end to the other end of the sample. Even in the presence of quantum tunneling, the metal-insulator transition is very close to this point. At higher surface coverage, the film is mostly metallic with voids of irregular shape, and finally the film becomes continuous.

The optical properties of such films show anomalous phenomena, which are absent both in the bulk metal and in the insulator. An anomalous resonant absorption peak is found in the visible or near-infrared (ir) regime, giving rise to anomalous behavior both in the transmittance and in the reflectance of these films.<sup>1–9</sup> In the ir regime, the transmittance of these films is much higher than that of a continuous metal film, while the reflectance is much lower. Close to the metal-insulator crossover, and well

before and after it, additional absorption is found, which can be as high as 40%.<sup>10</sup>

Several effective-medium theories were proposed for the optical properties of such films, based on the static approximation. The simplest descriptions, where exact information on the microgeometry is not needed, are the Maxwell-Garnett (MG),<sup>11</sup> the Bruggemann (BR),<sup>12</sup> and modifications of these two approaches. Good agreement with experimental results is found as long as the filling factor (metal volume fraction for cermets and percentage of surface coverage for semicontinuous metal films) is either very low or very close to 1, i.e., either a small quantity of metallic grains embedded in an insulating matrix or a small quantity of insulating grains embedded in a metallic matrix. As the filling factor approaches the intermediate value where a metal-insulator transition occurs, the measured absorption peak becomes wider than the calculated one, and the ir transmittance and reflectance deviate from the predicted values. The discrepancies are especially large close to the metal-insulator transition, even when the component parameters are adjusted and allowed to assume unphysical values.

Optical properties of discontinuous gold films<sup>2,3</sup> are in good agreement with the MG theory for very low filling factors, and worse for larger ones. The measured absorption peak is wider than the MG one, and the ir transmittance is much lower than the calculated value. Measurements on Au-SiO<sub>2</sub> and Ag-SiO<sub>2</sub> mixtures are in reasonable agreement with modified MG theories<sup>1</sup> for metal-rich or insulator-rich samples, but large discrepancies are found near the metal-insulator transition, especially in the ir. Fitting of Pt-Al<sub>2</sub>O<sub>3</sub> data to both MG and BR theories near the metal-insulator transition shows that the BR theory is more applicable,<sup>4</sup> as the two com-

ponents (metal and insulator) play a similar role. In this case, good agreement between theory and experiment was found over a wide range of filling factors; yet the agreement close to the percolation threshold was poor, and unphysical parameter values had to be used in the fitting process.

Investigation of a number of percolating films<sup>5-9</sup> very close to the percolation threshold show the following common properties: (1) a very weak wavelength dependence in the near-ir regime, (2) the transmittance decreasing linearly with increasing filling factor, while the reflectance exhibits the opposite trend, and (3) metallic to dielectric crossover observed in optical behavior only for long enough wavelengths (at smaller wavelengths, one cannot differentiate between “metallic” and “dielectric” films that are very close to the electrical percolation threshold).

Recently Yagil and Deutscher suggested another approach to the understanding of optical properties near the percolation threshold,<sup>13</sup> based on the inhomogeneity of a percolating film on length scales smaller than the percolation correlation length. In that description, the optical properties, i.e., reflectance, transmittance and absorbance, constitute a measurement on a typical length scale of size  $L(\omega)$ . Each area of this linear size is either metallic or dielectric, and the optical response of the whole film can be obtained by summing over these local contributions. Using this approach, the optical properties described above are recovered, at least qualitatively. A quantitative model, based on the experimental results of Gadenne *et al.*<sup>6,7,10</sup> but applicable only to the optical reflectance, was recently suggested by Robin and Souillard.<sup>14</sup> In that calculation similar scaling assumptions are made, and the reflectance of a single cluster is calculated in a simplified model. A detailed quantitative theory with which the reflectance, the transmittance, and the absorbance can be consistently calculated is still lacking.

In this study we apply the scaling theory of percolating random resistor networks to describe the optical properties of thin semicontinuous metal films: We calculate the effective (complex) conductivity and show that at finite frequencies it fluctuates over the film. The length scale of the fluctuating regions is determined by the anomalous diffusion relation. We find that the fluctuations are described by a wide bimodal distribution function. The average effective conductivity calculated from this distribution differs significantly from the most probable value. Therefore, instead of using a single average effective conductivity, we use the local effective conductivities to calculate the local optical properties, such as the local absorption. The total absorption is then found by averaging the local contributions. In the range of filling factors where the fluctuations are unimportant (far from the percolation threshold), our model is in agreement with the simple effective-medium theories at long wavelengths. At shorter wavelengths, where the MG resonance occurs, our model could and should be modified to include this phenomena. In the range of wavelengths that we have focused upon ( $\lambda \geq 1.5 \mu\text{m}$ ), and in the not extremely dilute case (metal fraction  $\geq 0.1$ ), that resonance is unimportant, and therefore we have ignored it. From our calcula-

tions, we conclude that over a wide range of filling factors around the percolation threshold, the optical properties are dominated by the fluctuations and, therefore, cannot be described by a simple effective dielectric constant. We show that the intercluster capacitance plays an important role in determining the optical response of a percolative film. Excellent agreement is found between the experimental data and a numerical calculation based on our model.

The rest of this article is organized as follows: In Sec. II we describe the optical properties of thin homogeneous films and review the effective-medium theories. In Sec. III we describe this model in detail. Comparison with experimental results is shown in Sec. IV and the conclusions are given in Sec. V.

## II. EFFECTIVE MEDIUM THEORIES

There are two effective-medium theories commonly used to describe electromagnetic properties of heterogeneous media. The first one, known as the Maxwell-Garnett theory (MG),<sup>11</sup> is applicable in composites consisting of spherical grains of one component embedded in a matrix of the other component. In the MG approach one considers an average cell consisting of a spherical inclusion covered by a layer of host so that in each such cell a proper filling factor  $f$  is maintained. In an external electric field, a dipole moment is induced on the inclusion. The effective dielectric constant is then determined by the requirement that when the average cell is replaced by a sphere of the same volume completely filled by the effective medium, the induced dipole moment remains unchanged. This procedure, using the static dipole induced on a dielectric sphere, leads to the following equation for the effective dielectric constant  $\epsilon_{\text{MG}}$ :

$$\frac{\epsilon_{\text{MG}} - \epsilon_2}{\epsilon_{\text{MG}} + 2\epsilon_2} = f \frac{\epsilon_1 - \epsilon_2}{\epsilon_1 + 2\epsilon_2}, \quad (2.1)$$

where  $\epsilon_1$  and  $\epsilon_2$  are the dielectric constants of the inclusion and the host respectively.

Since the first appearance of the MG theory, various corrections to its simple form have been studied extensively. In particular, Cohen *et al.*<sup>1</sup> have considered ellipsoidal inclusions, Bergman<sup>15,16</sup> and Kantor and Bergman<sup>17</sup> have examined contributions of higher multiple moments. Bedeaux and Vlieger<sup>18</sup> extended MG theory treatment to a two-dimensional layer of spheres, and Bobbert and Vlieger<sup>19</sup> discussed the interaction of this layer with the substrate.

If all of these corrections are taken into account, MG theory gives reasonable agreement with experiment, provided that its basic assumptions hold, i.e., one component is present in the form of small spherical or nearly spherical inclusions. At higher volume fractions of this component, when it starts to form clusters of irregular shape, MG theory yields a calculated transmittance that is much higher than observed in experiment. The disagreement between MG and experiment is strongest close to the percolation threshold, where both metal and insulator form large clusters and no clear distinction between “host” and “inclusions” can be made.

A more symmetrical description, the Bruggemann<sup>12</sup> effective-medium theory (BR), seems to be better near the percolation threshold. In the BR model, both components are assumed to be present as small spheres embedded in the supposedly uniform effective medium with volume fractions  $f$  and  $1-f$ , respectively. The condition that the total dipole moment induced in these spheres vanishes leads to the equation

$$f \frac{\epsilon_1 - \epsilon_{BR}}{\epsilon_1 + 2\epsilon_{BR}} + (1-f) \frac{\epsilon_2 - \epsilon_{BR}}{\epsilon_2 + 2\epsilon_{BR}} = 0. \quad (2.2)$$

Both the MG theory and the BR theory are long-wavelength approximations: They assume that the wavelength is much larger than any other length scale in the system. This assumption is not always satisfied, since the relevant wavelength is that inside the medium which is given by  $\lambda_0/\sqrt{\epsilon_e}$ , where  $\lambda_0$  is the wavelength in vacuum and  $\epsilon_e$  is the bulk effective dielectric constant of the mixture. This can turn out to be much smaller than the wavelength in the pure insulator. In fact, when applied to semicontinuous metal films, BR typically yields an effective wavelength (skin depth) comparable to the film thickness, which is the *smallest* length scale. We conclude, therefore, that any application of MG or BR theories and their modifications is inherently inconsistent close to the percolation threshold.

We present now a brief summary of the optical properties of a homogeneous metal film. The complex dielectric constant of a metal is connected to its dc conductivity  $\sigma_{dc}$  via the Drude formula:

$$\epsilon = \epsilon_0 + i \frac{4\pi\sigma_{dc}}{\omega(1+i\omega\tau)}, \quad (2.3)$$

where  $\tau$  is the relaxation time. In the case of an incident wave normal to the film surface, the reflection and transmission amplitudes are given by<sup>20</sup>

$$r = -x \frac{1 - e^{2iKd}}{1 - x^2 e^{2iKd}}, \quad (2.4a)$$

$$t = \frac{1 - x^2}{1 - x^2 e^{2iKd}} e^{i(K-k)d}, \quad (2.4b)$$

where  $x = (K-k)/(K+k)$ ,  $k = \omega/c$ ,  $K$  is the complex wave number inside the film  $K = (\sqrt{\epsilon})\omega/c$ , and  $d$  is the film thickness. Reflectance, transmittance and absorptance of a 100-Å-thick metal film as a function of its dc conductivity are plotted in Fig. 1.

In the long-wavelength limit when  $\omega\tau \ll 1$ ,  $Kd \ll 1$ , and  $\omega \ll \sigma_{dc}$ , the reflected and transmitted amplitudes reduce to

$$r = -\frac{1}{1 + \frac{c}{2\pi d \sigma_{dc}}}, \quad (2.5a)$$

$$t = \frac{1}{1 + \frac{2\pi d \sigma_{dc}}{c}}. \quad (2.5b)$$

Notice that these expressions do not depend on the wavelength. In the effective-medium description, the effective

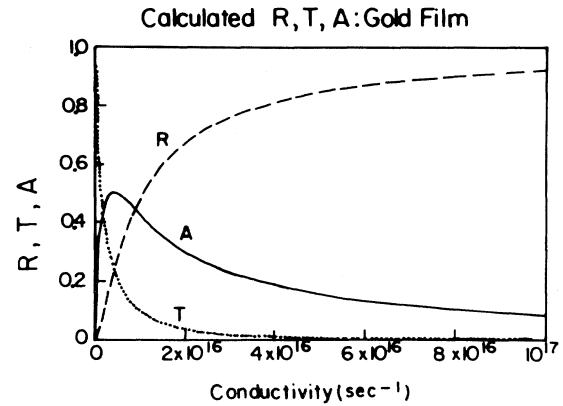


FIG. 1. Reflectance, transmittance, and absorptance of a homogeneous Drude metal film versus dc conductivity for a wavelength of  $2.5 \mu\text{m}$ . The conductivity of a bulk Au film is  $3.5 \times 10^{17} \text{ sec}^{-1}$ . This graph was calculated using the exact formulas of (2.4). We have checked and found that if we use instead the approximate formula (2.5), the results change by at most a few percent.

dc conductivity is a function of the volume fraction  $f$ . As  $f$  varies from 0 to 1,  $\sigma_{dc}$  changes by many orders of magnitude, approaching the bulk metallic conductivity ( $3.5 \times 10^{17} \text{ sec}^{-1}$  for gold). From (2.5) it follows that there is a sharp crossover from insulating behavior ( $|r| \ll 1$ ,  $|t| \approx 1$ ) to metallic behavior ( $|t| \ll 1$ ,  $|r| \approx 1$ ) when  $\sigma_{dc}$  approaches  $c/2\pi d$ . For a 100-Å-thick film, this crossover occurs when  $\sigma_{dc} \approx 5 \times 10^{15} \text{ sec}^{-1}$  (Fig. 1). We note that although (2.5) is not valid for all values of  $\omega$  and  $\sigma$ , we have verified that it is a good approximation throughout the crossover region. Typically, when the effective dc conductivity of the composite is used in (2.5), the predicted crossover with  $f$  is much sharper than observed in experiment.<sup>10</sup> Unphysical values of various parameters are usually required in order to broaden the predicted transition.

### III. SCALING THEORY

Transmission electron micrographs (TEM's) of a typical semicontinuous metal film reveal an irregular network of metal grains forming large ramified clusters. The cluster sizes are characterized by the percolation correlation length  $\xi$ , which diverges when the surface-coverage parameter  $p$  approaches the critical value  $p_c$ . At length scales smaller than  $\xi$ , both the metal clusters and the insulator (void) clusters separating them have a similar fractal structure. The scaling theory of electric transport on percolating networks has been studied extensively in recent years.<sup>21-37</sup> It was found that on length scales much larger than  $\xi$ , the film appears homogeneous and its conductivity is size independent. On the other hand, if one measures the conductivity of a small piece of the film of linear size smaller than  $\xi$ , the measured value differs for different pieces of the same film and its average value depends on the size of the measured pieces. These fluctuations reflect the inhomogeneous nature of the frac-

tal network on length scales shorter than the percolation correlation length. The average conductivity obtained from a large number of measurements is length dependent and increases as the pieces size decreases. It must be emphasized that the average conductivity cannot give a complete description of the optical properties of percolating films, since the dependence of the absorption on the conductivity is strongly nonlinear, as shown in the previous section. The absorption depends, therefore, on the precise shape of the conductivity distribution and not only on the average conductivity.

A dc measurement probes the conductivity on a length scale determined by the sample size. Measuring at a finite frequency  $\omega$  introduces an additional length scale  $L(\omega)$ . Optical measurements are thus a finite-size probe, where the ac conductivity is measured over this length scale. Several approaches have been used to determine the dependence of  $L(\omega)$  on  $\omega$ . In the anomalous diffusion picture,<sup>38</sup> a random walk on the percolation backbone is considered. Due to the fractal nature of the percolating network, the mean-square distance traveled by a random walker scales with the travel time  $t$  as

$$\langle r^2(t) \rangle \sim t^{2/(2+\theta)}, \quad (3.1)$$

where  $2+\theta$  is the fractal dimension of the random walk. For a homogeneous system,  $\theta=0$  and (3.1) gives the usual linear dependence of the mean-square distance on the travel time. For the two-dimensional percolation problem, the scaling theory gives  $\theta=(\mu-\beta)/\nu=0.79$ . The frequency  $\omega$  of the applied field determines the travel time  $t$ . During this period of time, the random walker traverses a region of finite linear size given by

$$L(\omega) = B \xi_0 (\lambda/\xi_0)^{1/(2+\theta)} \sim \omega^{-1/(2+\theta)}, \quad (3.2)$$

where  $\lambda$  is the wavelength,  $B$  is a coefficient of order 1, and  $\xi_0$  is defined by (3.5) below.

The anomalous diffusion picture assumes that the random walker travels on a single cluster whose size is larger than  $L(\omega)$ . In the case of ac current, the above relation is valid as long as all capacitance-related impedances are much larger than that of the metallic path.

The conductivity and capacitance of this finite region can be very different from the long-length-scale conductivity and capacitance measured over the entire film. Moreover, at length scales shorter than the percolation correlation length, the electrical properties of a finite-size region are different at different locations in the same film.

The average conductivity of a good-conductor-bad-conductor mixture of linear size  $L$ , near the percolation threshold of the good conductor, is given by<sup>39</sup>

$$\sigma_{av} = \sigma_m L^{-\mu/\nu} F((\sigma_i/\sigma_m) L^{(\mu+s)/\nu}), \quad (3.3)$$

where  $\sigma_m$  and  $\sigma_i$  are the conductivities of the good and the bad conductor, respectively. This expression was proposed originally for the case of dc conductivity but can be used also to describe ac conductivity. In that case both  $\sigma_m$  and  $\sigma_i$  will be complex. All the lengths are measured in units of the typical grain size  $a_0$ , thus both  $L$  and the correlation length  $\xi$  are dimensionless. The scaling function  $F(z)$  has the following limiting forms.<sup>26,39,40</sup>

For large values of  $|z|$ , the form is

$$F(z) = A_0 z^{\mu/(\mu+s)}, \quad |z| \gg 1, \quad (3.4a)$$

but for small  $|z|$ , the form depends upon whether there exists a conducting path connecting opposite sides of the sample. If such a path exists, then

$$F(z) = A_1 + A_2 z, \quad |z| \ll 1 \text{ (metallic behavior)}. \quad (3.4b)$$

In this case, the conductivity is determined mainly by the metal and the dielectric properties of the insulator only provide a small correction. If there is no conducting path across the sample, then

$$F(z) = A_3 z + A_4 z^2, \quad |z| \ll 1 \text{ (dielectric behavior)}, \quad (3.4c)$$

and the sample is insulating for a dc signal. In other words, at intermediate length scales, where  $|(\sigma_i/\sigma_m) L^{(\mu+s)/\nu}| \ll 1$ , there is a clear distinction between conducting and insulating parts of a fractal, whereas at very large scales where  $|(\sigma_i/\sigma_m) L^{(\mu+s)/\nu}| \gg 1$ , the existence of a conducting path becomes unimportant and the conductivity is given by Eqs. (3.3) and (3.4a).

The exponent  $\nu$  in (3.3) determines the scaling behavior of the percolation correlation length as  $p$  approaches  $p_c$ ,

$$\xi = \xi_0 |p - p_c|^{-\nu}; \quad (3.5)$$

$\mu$  and  $s$  are the dc conductivity and capacitance exponents, respectively ( $s$  is also the superconductivity exponent, for a metal-superconductor mixture). In simple percolating systems (e.g., a binary random-resistor network), all the critical exponents appearing in (3.3) have universal values that depend only on the dimensionality of the system. In two dimensions, the critical exponents have the values  $\nu = \frac{4}{3}$  and  $\mu = s = 1.3$ , both in site and bond percolation. Continuum percolation may cause some changes in these values, as will be discussed in the next section.

The nonuniversal coefficients, such as  $\xi_0$ ,  $p_c$  and  $A_0, \dots, A_4$  depend on the details of the microgeometry. Their values cannot be determined from the scaling theory of percolation and must be adjusted to the particular system in question.

The simple scaling expression (3.3) is valid only as long as  $L$  is smaller than the correlation length  $\xi$ . At length scales much larger than  $\xi$ , the network is homogeneous and its conductivity is governed by  $\xi$ , rather than by  $L$ :

$$\sigma_{av} = \sigma_m \xi^{-\mu/\nu} F((\sigma_i/\sigma_m) \xi^{(\mu+s)/\nu}), \quad L \gg \xi. \quad (3.6)$$

It seems therefore desirable to introduce the effective length scale  $L_\xi$ , with the following properties:

$$L_\xi = \begin{cases} L(\omega) & L(\omega) \ll \xi \\ \xi & L(\omega) \gg \xi \end{cases}. \quad (3.7)$$

Now one can represent the conductivity in a form valid on any length scale:

$$\sigma_{av} = \sigma_m L_\xi^{-\mu/\nu} F((\sigma_i/\sigma_m) L_\xi^{(\mu+s)/\nu}). \quad (3.8)$$

This form is equivalent to the usual representation of the conductivity as a function of *two* scaling variables:<sup>39</sup>

$$\sigma_{av} = \sigma_m L^{-\mu/\nu} \bar{F}((\sigma_i/\sigma_m)L^{(\mu+s)/\nu}, L/\xi). \quad (3.9)$$

We turn now to the discussion of the conductivity fluctuations. Consider first a mixture of conductor with specific conductivity  $\sigma_0$  and perfect insulator ( $\sigma=0$ ), divided into a set of squares of linear size  $L$ . A fraction  $f$  of these squares will have a conducting path connecting opposite sides. The dc conductivity of all squares that do not have such a path is equal to zero. Therefore, the dc conductivity distribution function can be broken into two parts:

$$P(\sigma) = (1-f)\delta(\sigma) + fP(\sigma; L, \sigma_0, \xi), \quad (3.10)$$

where  $P(\sigma; L, \sigma_0, \xi)$  describes the distribution of conductivities of conducting squares.

Near the percolation threshold, where  $L/\xi \ll 1$ , the probability  $f$  of finding a conducting square has the following scaling properties:<sup>41</sup>

$$f - f_c \sim \pm (L/\xi)^{1/\nu}, \quad (3.11)$$

where  $f_c$  is the value of  $f$  at  $p=p_c$ . For self-dual lattices,  $f_c = \frac{1}{2}$ . If the dual symmetry is broken, as usually happens in continuum percolation, the correlation length is equal to  $\xi_0^{(+)}|p-p_c|^{-\nu}$  above  $p_c$  and to  $\xi_0^{(-)}|p-p_c|^{-\nu}$  below  $p_c$ . Inserting these expressions for  $\xi$  into (3.11), we find

$$f - f_c = u_{\pm} [L/\xi_0^{(\pm)}]^{1/\nu} (p - p_c). \quad (3.12)$$

Since the slope of  $f$  must be continuous at  $p=p_c$ , the coefficients  $u_{\pm}$  must satisfy

$$\frac{u_+}{u_-} = \left[ \frac{\xi_0^{(+)}}{\xi_0^{(-)}} \right]^{1/\nu}.$$

The scaling relation (3.11) holds only if  $L \ll \xi$ . In order to avoid introduction of an additional scaling function  $f(L, \xi)$ , we will make the following ansatz. We assume that Eq. (3.12) is valid for arbitrary values of  $L$  and  $\xi$ , provided that  $L$  is replaced by  $L_{\xi}$ . One can easily check that, for  $L \gg \xi$ , correct limits are obtained if we make the following choice of parameters:

$$f_c = \frac{(\xi^{(-)})^{1/\nu}}{(\xi^{(+)}|p-p_c|^{-\nu})^{1/\nu} + (\xi^{(-)})^{1/\nu}},$$

$$u_- = f_c,$$

$$u_+ = 1 - f_c.$$

This ansatz differs from all the other scaling assumptions made in connection with the percolation problem: It allows us to use a simple expression, namely, (3.12) to describe the entire range of possible values of  $f$ , by the use of a single variable length scale  $L_{\xi}$ .

The probability distribution  $P(\sigma; L, \sigma_0, \xi)$  has been studied in some detail only at  $p=p_c$  (infinite  $\xi$ ), by considering an ensemble of samples of linear size  $L$ . A computer simulation by Rammal, Lemieux, and Tremblay<sup>42</sup> has shown that this distribution scales with the sample

size as  $L^{-\mu/\nu}$ . This result, together with the homogeneity of the distribution,<sup>43</sup> implies that at  $p_c$  the probability distribution can be written as a function of a single scaling variable  $z = \sigma/\sigma_{av}(L)$ . The resulting distribution  $P_c(z)$  is *universal*, i.e., it does not depend either on the length scale or on the details of the underlying lattice. Since  $P_c(z)$  has been studied numerically,<sup>42</sup> we will treat it as a known function. If  $p \neq p_c$ , the distribution of  $z$  depends also on the size of the squares, which we will take to be  $L(\omega)$ : When  $L(\omega)/\xi \ll 1$ , the distribution  $P(z; L(\omega)/\xi)$  reduces to  $P_c(z)$ , but in the opposite limit  $L(\omega)/\xi \gg 1$ ,  $\langle \Delta\sigma^2 \rangle / \langle \sigma \rangle^2 \sim [L(\omega)/\xi]^{-2}$ , and  $P(z; L(\omega)/\xi)$  is then a Gaussian distribution whose width scales as  $[L(\omega)/\xi]^{-1}$ . Note that  $L(\omega)$  is used here and not  $L_{\xi}$  so that when  $L(\omega) \gg \xi$ ,  $P(z, L(\omega)/\xi)$  tends to a  $\delta$  function.

Consider now the expectation value of some physical quantity which depends on the dc conductivity, e.g., the absorptance  $A(\sigma)$ . We can replace integration over  $\sigma$  by integration over  $z = \sigma/\sigma_{av}(L_{\xi})$ , obtaining

$$A = f_c \int A(\sigma_{av}(L_{\xi} z^{-\nu/\mu})) P_c(z) dz, \quad p = p_c, \quad (3.13)$$

where  $\sigma_{av}(L_{\xi}) = \sigma_0 L_{\xi}^{-\mu/\nu}$ . Since  $A(\sigma=0) = 0$ , only the conducting squares give a nonzero contribution. Equation (3.13) gives the absorptance at  $p=p_c$ . A reasonable generalization of (3.13) to arbitrary values of  $p$  is

$$A = f \int A(\sigma_{av}(L_{\xi} z^{-\nu/\mu})) P(z; L(\omega)/\xi) dz, \quad (3.14)$$

where, in general,  $z$  is complex and the integration is two dimensional.

If the specific conductivities of the two components differ by several orders of magnitude, as in the case of metal-insulator films, it is still possible to distinguish between metallic and dielectric squares. We will assume that the contribution of the metallic squares to the expectation value of  $A(\sigma)$  is still given by (3.14), where  $\sigma_{av}$  is now determined by (3.8) and (3.4b). Although their dc conductivity vanishes, the dielectric squares have nonzero ac conductivity, so that their contribution to the absorption cannot be neglected. It is reasonable to assume that the absorption in the dielectric squares can be calculated by replacing  $f$  by  $1-f$  in (3.14) and taking  $\sigma_{av}$  from (3.8) and (3.4c). The total absorptance is thus calculated from

$$A = f \int A(\sigma_{av(m)}(L_{\xi} z^{-\nu/\mu})) P_m(z; L(\omega)/\xi) dz$$

$$+ (1-f) \int A(\sigma_{av(i)}(L_{\xi} z^{-\nu/\mu})) P_i(z; L(\omega)/\xi) dz, \quad (3.15)$$

where  $P_m$  and  $P_i$  are the distribution functions of the metallic and dielectric complex conductivities, respectively, and may be reasonably described by the real function  $P(z; L(\omega)/\xi)$  of Ref. 42.

#### IV. COMPARISON WITH EXPERIMENTAL RESULTS

In this section we present a comparison of the model with recent experimental results. The experimental data obtained by Gadenne, Yagil, and Deutscher<sup>10</sup> provide

most of the data needed for this comparison. The optical properties of semicontinuous gold films were measured during the growth process at two different wavelengths: 1.7 and 2.2  $\mu\text{m}$ . The data include reflectance, transmittance, and absorbance over the entire surface coverage range. In the regime that we investigated, the film consists of metallic islands whose vertical thickness stays approximately constant as more gold is deposited. It is the lateral dimension of the grains, as well as their total number, which increases, and along with them the fraction of surface covered by the metal. The nominal thickness is characterized by the mass of gold per unit area,  $D$ , as measured with the help of a piezoelectric monitor upon which an identical film is simultaneously deposited. The critical value of  $D$  at which the film begins to conduct electricity is denoted by  $D_c$ . The corresponding fractions of surface covered by metal are denoted by  $p$  and  $p_c$ . Experimental results<sup>10</sup> show that the normalized mass-thickness parameter  $\delta D = (D - D_c) / D_c$  is approximately equal to the normalized surface-coverage parameter  $\delta p = (p - p_c) / p_c$ . The experimental curves thus provide the dependence of the optical properties on the surface-coverage parameter.

Figure 2 shows the reflectance and transmittance of the Au film as measured, i.e., the optical properties of the film together with the glass substrate. A sharp drop in the optical transmittance is found already well below the percolation threshold, where the reflectance is changing much more slowly. Near the percolation threshold, both the reflectance and the transmittance are linear in  $\delta D$  and are weakly wavelength dependent. Well above the threshold, the reflectance increases rapidly and the transmittance becomes low, approaching the typical response of a homogeneous metal film. Close to the percolation threshold, and over a wide range before and after it, strong optical absorption is observed, as shown in Fig. 3 (in this case the substrate effect is excluded, as the

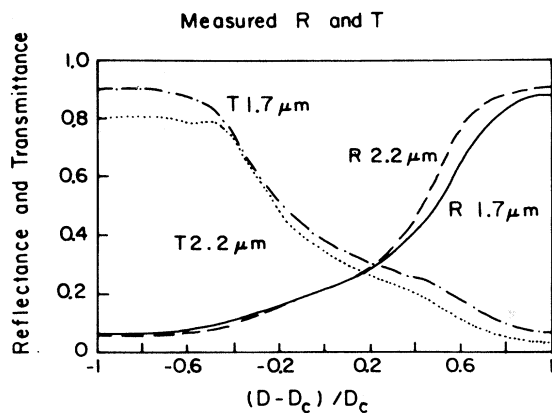


FIG. 2. Measured reflectance and transmittance of a semicontinuous Au film at 1.7 and 2.2  $\mu\text{m}$  as a function of the thickness parameter  $\delta D = (D - D_c) / D_c \approx (p - p_c) / p_c$  (from Ref. 10). The data include the substrate effect. At 2.2  $\mu\text{m}$  the substrate is absorbing, the transmittance is thus lower than the 1.7- $\mu\text{m}$  values.

borosilicate glass is absorbing at 2.2  $\mu\text{m}$ ). This strong absorption is observed in the regime where both the reflectance and transmittance are low and depend linearly on the surface coverage.

Calculation of the optical properties using our scaling model requires several assumptions for the unknown scaling functions. In the following, a brief description of the parameters and function used in our calculation is given.

The film consists of metal clusters separated by vacuum, thus the two basic ac conductivities have the forms

$$\sigma_1 = \sigma_{dc} / (1 - i\omega\tau), \quad (4.1)$$

$$\sigma_2 = -i\omega C_0, \quad (4.2)$$

where  $\sigma_{dc}$  is the dc conductivity of a continuous metal film,  $\tau$  is the relaxation time inside the metal grains (normally shorter than the bulk value), and  $C_0$  is of the order of the capacitance per unit thickness between two adjacent metal grains. Interband transitions are unimportant above 0.6  $\mu\text{m}$  (2 eV).<sup>44</sup>

The characteristic length  $L_\xi$  equals  $L(\omega)$  for  $L(\omega) < \xi$  and to  $\xi$  for  $L(\omega) > \xi$ , with a parabolic smoothing func-

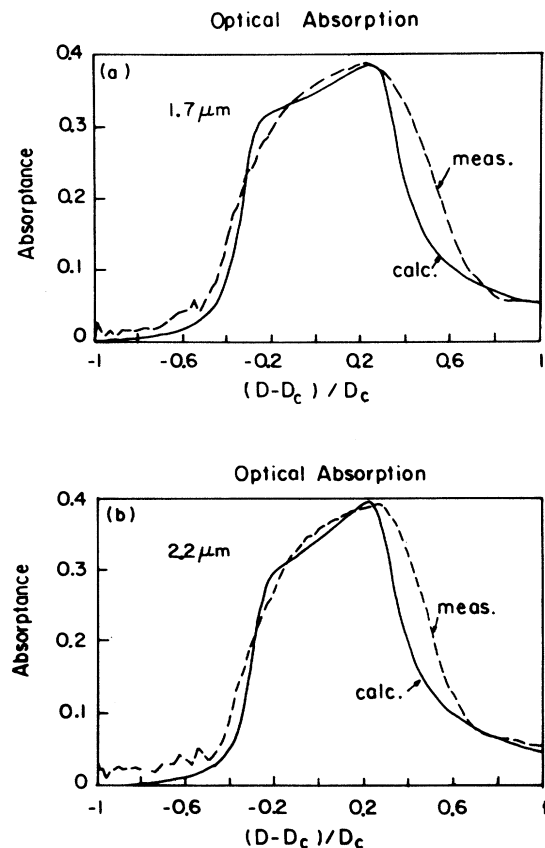


FIG. 3. Measured (from Ref. 10) and calculated absorbance of a semicontinuous Au film (i.e., the fraction of incident radiation that is absorbed by the film) as a function of the thickness parameter  $\delta D$ . The microgeometry of the actual films for  $0.3 \leq \delta D \leq 0.6$  is of long and narrow cracks rather than granular voids, as assumed by the model, resulting in enhanced absorption. (a)  $\lambda = 1.7 \mu\text{m}$ . (b)  $\lambda = 2.2 \mu\text{m}$ .

tion at  $L(\omega) \simeq \xi$ . Using the anomalous diffusion relation (3.2) and the scaling relations (3.4) and (3.8), we get the following results for the metallic and dielectric conductivities at the length scale  $L = L_\xi$ :

$$\begin{aligned} \sigma_m(L) &= \frac{A_1 \sigma_{dc}}{1 + \omega^2 \tau^2} L^{-\mu/\nu} \\ &+ i \left[ \frac{A_1 \sigma_{dc} \omega \tau}{1 + \omega^2 \tau^2} L^{-\mu/\nu} - A_2 C_0 \omega L^{s/\nu} \right], \quad (4.3) \\ \sigma_i(L) &= \frac{A_3 \omega^2 C_0^2}{\sigma_{dc}} L^{(\mu+2s)/\nu} \\ &+ i \left[ \frac{A_3 \omega^2 C_0^2 \omega \tau}{\sigma_{dc}} L^{(\mu+2s)/\nu} - A_4 C_0 \omega L^{s/\nu} \right]. \quad (4.4) \end{aligned}$$

These are used to obtain the complex dielectric constant as

$$\epsilon = \epsilon_0 + i \frac{4\pi\sigma}{\omega}, \quad (4.5)$$

where  $\epsilon_0$  is the ionic contribution to the dielectric constant. Dividing the film into squares of linear size  $L_\xi$  and different values of  $\epsilon$ , the reflectance and transmittance of each square is calculated using the formulas for a thin homogeneous film with the same dielectric constant. The optical response of the whole film is then given by the generalized relation (3.15), where the distribution functions  $P_m(z, L(\omega)/\xi)$  and  $P_i(z, L(\omega)/\xi)$  are unknown. We have assumed that both of these functions in the ac case have the same form that was found by Rammal *et al.* for the dc case.<sup>42</sup> We use this function in (3.15), where  $z$  is a real variable, even though the local conductivities that appear there are complex. The use of this function provides a proper coupling between the contributions of the metallic paths and the capacitive links, and the proper dc limit when the frequency vanishes. To simplify calculations, the distribution function of Rammal *et al.* is approximated by a log-normal distribution. The optical reflectance is thus given by

$$\begin{aligned} R &= f \int R_m(L_\xi z^{-\mu/\nu}) P_m(z; L(\omega)/\xi) dz \\ &+ (1-f) \int R_i(L_\xi z^{-\mu/\nu}) P_i(z; L(\omega)/\xi) dz, \quad (4.6) \end{aligned}$$

where  $R_m(L)$  and  $R_i(L)$  are the reflectance of a metallic and a dielectric square of linear size  $L$ , and  $f$ , is given by (3.12). The optical transmittance and absorbance are calculated in a similar form.

In general, the scattering amplitude would have to be calculated as function of the scattering angle. This calculation would yield both specular and nonspecular scattering, and would depend on the spatial correlation function of the fluctuating local conductivity (analogous to the form factor). In our case, the nonspecular scattering is negligible,<sup>10</sup> experimentally. This means that the only important Fourier components of the correlation function have either  $q \simeq 0$  (the transmitted wave) or  $q \simeq 2$  times the normal component of the incident wave vector

(the specularly reflected wave). In this situation the total absorption coefficient is correctly calculated by summing the local absorption coefficients from all parts of the film, as done in (3.15). But in order to calculate the specular reflection and transmission coefficients we would have to integrate the scattered field from the different parts of the film before calculating the scattered intensity, which would depend on the above mentioned correlation function. This would be a very difficult undertaking, since the length scales of the inhomogeneity are neither uniformly small nor uniformly large compared either with the wavelength or with the skin depth. Moreover, the film thickness as well as the skin depth are so small that one is really in the regime of the anomalous skin effect, where the use of a local conductivity  $\sigma$  is strictly invalid. We therefore calculated the total reflectance coefficient by integrating its "local value" over the film, using (4.6): The local reflectance coefficient was calculated using the local value of  $\sigma$ , as though we had a uniform film with that value of  $\sigma$ .

A similar procedure was used to calculate the total transmittance coefficient. At present, we are unable to provide a full justification for this procedure, except in the calculation of the total absorption coefficient. It is nevertheless striking that we can get such good agreement with experiment, as we show below.

Although there are no fitting parameters in our model, the comparison to experimental results is somewhat delicate, as some of the physical parameters and all the scaling function coefficients are unknown. In principle, all the physical parameters could be measured separately, by nonoptical measurements, and the coefficients of the scaling functions could thus be obtained. In the comparison with the results of Gadenne, Yagil, and Deutscher, some of these values were indeed estimated in this way, while others had to be adjusted using the optical measurements.

From the experimental data, the critical mass thickness  $D_c$  equals 75 Å, a typical grain size (channel width) is 300 Å, the physical thickness of the film is 100 Å, and the bulk dc conductivity equals  $3 \times 10^{17} \text{ sec}^{-1}$ . The value found for the conductivity exponent  $\mu$  was 1.43 rather than the theoretical one (1.3). This is interpreted as due to the continuum percolation character of the samples, as discussed by Halperin *et al.*<sup>45</sup> The optical relaxation time  $\tau$  was determined by adjusting the calculated values of  $A$  and  $R$  to the measured values, using the functional form of Theye:<sup>44</sup>  $1/\tau = 1/\tau_0 + b\omega^2$ . The values of  $\tau$  found in this way are of the order of  $2 \times 10^{-15} \text{ sec}$ , which is smaller than the electrical relaxation time and is wavelength dependent. In the experimental data of Ref. 10,  $\text{Im}(\epsilon)$  of the continuous film is larger than the values reported by Theye, thus the relaxation time should indeed be shorter. For a single capacitive link,  $C_0$  is of order unity, since the separation between two adjacent grains, the grain size, and the film thickness are all of the same order.

The width of the distribution function for the local ac conductivity was taken as 0.3, for best fit with the distribution reported by Rammal *et al.*<sup>42</sup> The coefficients  $A_1, A_2, A_3$ , and  $A_4$  in (3.4) and  $B$  of (3.2) are of order unity.

Using the above relations and constants, the optical properties of films similar to those measured by Gadenne *et al.* can be calculated for arbitrary surface coverage parameter and wavelength. Use of the anomalous diffusion relation restricts this calculation to the regime where both  $|\sigma_2/\sigma_1|$  and  $|\sigma_i/\sigma_m|$  are small. For the highest frequency used here ( $\lambda=1.7 \mu\text{m}$ ,  $\omega=1.1 \times 10^{15}$ ), these two quantities are 0.015 and 0.35, respectively. At lower frequencies  $|\sigma_2/\sigma_1|$  vanishes as  $\omega$  and  $|\sigma_i/\sigma_m|$  vanishes at least at  $\omega^{1/3}$ . We therefore do not expect a significant deviation from the anomalous diffusion picture due to the capacitive corrections.

The calculated absorption is shown in Fig. 3, together with experimental data. The agreement is excellent except for the range  $0.3 \leq \delta D \leq 0.6$ , where the measured absorption is somewhat higher than the calculated value. This will be discussed later. Close to the percolation threshold the correlation length is larger than the anomalous diffusion length  $L(\omega)$ , thus the optical properties are calculated over the length scale  $L(\omega)$ . Both the wide distribution of the local ac conductivities and the intercluster capacitance enhance the optical absorption. Strong absorption arises from parts of the film, where the local conductivity is moderate and the capacitance is appreciable. The wide region of strong absorption, both above and below the percolation threshold, is identified as the region where  $L(\omega) < \xi$ . This region is wide and depends weakly on the optical frequency because  $L(\omega)$  is much smaller than the optical wavelength, and only increases as a weak power of  $1/\omega$ , as given by the anomalous diffusion relation (3.2).

As  $\xi$  drops below  $L(\omega)$ , either above or below  $p_c$ , i.e., both in the metallic and in the dielectric regimes, the absorption decreases dramatically. In the dielectric case, the absorption is due to Joule losses in a metallic cluster which is connected to neighboring clusters by the intercluster capacitance. The current density in such a cluster is greater than what it would be in an isolated cluster, resulting in enhanced absorption. In the metallic regime, reduced conductivity together with a positive contribution to the real part of the dielectric constant, due to capacitance effect in the voids, enhance the absorption. Strong absorption is thus found whenever clustering occurs, on both the dielectric and the metallic wings of the percolation threshold.

In the range  $0.3 \leq \delta D \leq 0.6$ , the calculated absorption is somewhat lower than the measured one. The microgeometry in this regime deviates appreciably from the simple network percolation picture: Long and narrow cracks are found rather than small spherical voids, and these cracks become thinner with increasing surface coverage. The basic capacitive link  $C_0$  is thus not constant and increases with increasing surface coverage. In the above calculation,  $C_0$  was kept constant, resulting in a value for the film capacitance that is too low. Therefore the calculations presume a film that is more metallic than the actual film, and the calculated variation of the optical properties with  $p$  is thus too strong.

The experimental curves for the measured reflectance and transmittance contain the substrate effect, whereas the calculation was done for a free standing film. There-

fore, the comparison in this case is somewhat less quantitative. In particular, the borosilicate substrate is absorbing at  $2.2 \mu\text{m}$ , thus the measured transmittance for the low-surface-coverage regime in  $2.2 \mu\text{m}$  is lower than the value at  $1.7 \mu\text{m}$  (see Fig. 2), in contrast with the predicted behavior which is that the transmittance at  $2.2 \mu\text{m}$  is slightly higher than at  $1.7 \mu\text{m}$  (see Fig. 4). The calculated reflectance and transmittance are shown in Fig. 4, and the measured values in Fig. 2. As shown in these two graphs, the characteristic behaviors of both the reflectance and transmittance found in the experimental results are fully recovered. The transmittance shows a sharp change whenever clustering begins, a weak variation close to the percolation threshold with linear dependence on the surface-coverage parameter  $p$ , and a rather sharp drop to very low values in the metallic region. A similar behavior is found for the reflectance data: a sharp drop in the metallic region when dielectric clusters first appear, linear surface-coverage dependence close to  $p_c$ , and a rather sharp decrease in the dielectric region. As in the case of the absorptance, the calculated reflectance and transmittance in the nearly metallic regime are somewhat different from the experimental values, resulting from the details of the exact microgeometry.

Close to  $p_c$ , a linear surface-coverage dependence is found in both the transmittance and the reflectance. In our model, the optical properties in this regime depend on a constant length scale  $L_\xi = L(\omega) \ll \xi$ ,  $P_m$  and  $P_i$  reduce to the universal distribution function  $P_c$ , and (4.6) can be written in the form

$$R = f \int P_c(z, L(\omega)) R_m(z) dz + (1-f) \int P_c(z, L(\omega)) R_i(z) dz . \quad (4.7)$$

Since the two integrals depend only on  $L(\omega)$  and are independent of  $p$ , this relation reduces to that suggested by Yagil and Deutscher:<sup>13</sup>

$$R = f R'_m(L(\omega)) + (1-f) R'_i(L(\omega)) . \quad (4.8)$$

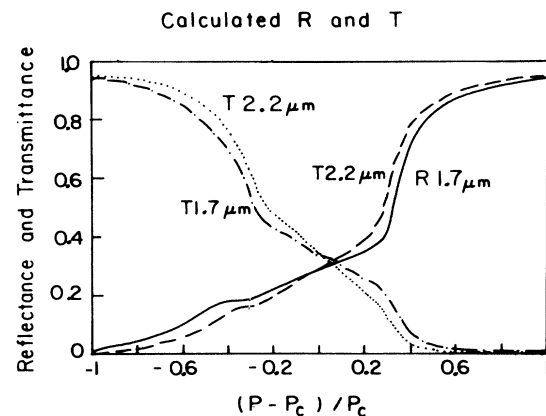


FIG. 4. Calculated reflectance and transmittance of a semicontinuous Au film at 1.7 and  $2.2 \mu\text{m}$  as a function of the coverage parameter  $\delta p$ . The data does not contain the substrate effect.



A similar relation holds for the transmittance. A linear dependence on the surface coverage is thus obtained as long as  $f$  is linear with  $p$ , which is the case close to  $p_c$  [see (3.12)].

For comparison, we show in Fig. 5 the results of applying Bruggemann's effective-medium approximation to calculate  $\epsilon_{\text{eff}}$  [see Eq. (2.2)] for this experiment, and then using that value in Eqs. (2.3) and (2.4) to calculate  $R$ ,  $T$ , and  $A$ . It is clear that this kind of approach cannot begin to explain the optical measurements.

Experimental data show that the transmittance and reflectance of films at  $p_c$  are constant in the range 1.5–2.5  $\mu\text{m}$ . The transmittance increases with wavelength for films slightly below  $p_c$  and decreases in the opposite case.<sup>5–9</sup> This behavior is fully recovered in our calculations, as shown in Fig. 6, using the parameters described above. A weak wavelength dependence is found as long as  $T'_i$ ,  $T'_m$ ,  $R'_i$ , and  $R'_m$  are only weakly wavelength dependent. This is the case in the range 1.5–2.5  $\mu\text{m}$ , where  $\omega\tau \approx 1$  and where these quantities are also nonmonotonic. For longer wavelengths, the calculated reflectance of a film at  $p_c$  decreases with increasing wavelength, while the transmittance increases. Changing the film parameters yields similar results, where the reflectance and transmittance can have arbitrary values and the weak wavelength dependence region can be extended up to 5  $\mu\text{m}$ .

The calculated optical properties at much longer wavelengths are shown in Fig. 7, using again the same parameters. At  $p_c$ , the reflectance decreases with increasing wavelength, in agreement with the scaling calculation performed by Robin and Souillard.<sup>14</sup> For  $p \neq p_c$ , the film becomes homogeneous at such long scales [ $\xi \ll L(\omega)$ ] and the model reduces to a Drude metal. As shown in Sec. II, a thin metallic film may have any value for  $R$ ,  $T$ , and  $A$ , depending on the product  $\sigma d$ , where  $\sigma$  is the dc conductivity and  $d$  is the film thickness. It is important to emphasize that at long wavelengths the relaxation time  $\tau$  and the capacitance effect are negligible, thus only the

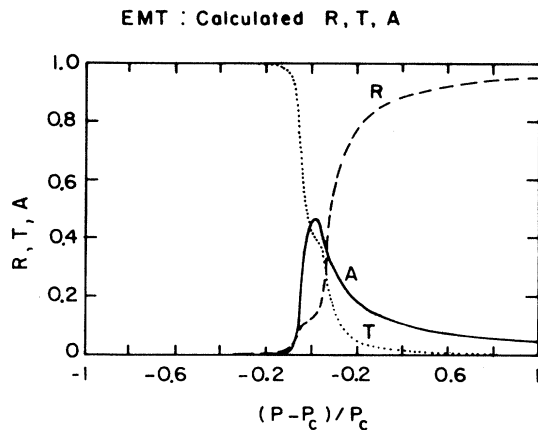


FIG. 5. Calculated reflectance, transmittance, and absorbance obtained from Bruggemann's effective-medium approximation at 2.2  $\mu\text{m}$ .

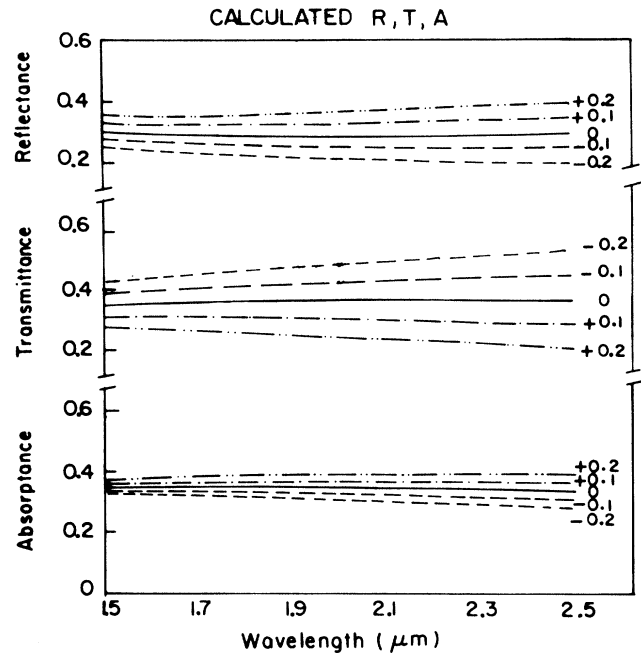


FIG. 6. Calculated reflectance, transmittance, and absorbance of semicontinuous Au films for several values of the coverage parameter  $\delta p$  as indicated on the graph, in the wavelength range 1.5–2.5  $\mu\text{m}$ .

dc conductivity controls the optical properties. When the film is absorbing, the optical properties become wavelength independent, as shown in Fig. 7, in agreement with the approximation discussed in Sec. II.

In summary, the calculated optical properties are in excellent agreement with the experimental data discussed above, and in general agreement with the experimental data on all percolating films close to the percolation threshold.

## V. CONCLUSIONS

In this model we have shown that for semicontinuous metal films close to the percolation threshold, when the anomalous diffusion length  $L(\omega)$  is smaller than the percolation correlation length  $\xi$ , a scaling description is more applicable than an effective-medium approach. The following points are important in calculating the optical properties.

(1) Optical measurements probe the film on a finite length scale  $L(\omega)$ . The local ac conductivity must be calculated using finite-size scaling on that length scale.

(2) On the scale of  $L(\omega)$ , the local ac conductivity fluctuates over the film, and a wide bimodal distribution must be used to describe these fluctuations.

(3) The metallic clusters are fractals, therefore  $L(\omega)$  depends on the optical frequency through the anomalous diffusion relation, and is much smaller than the optical wavelength.

(4) Intercluster capacitance gives rise to a nonzero con-

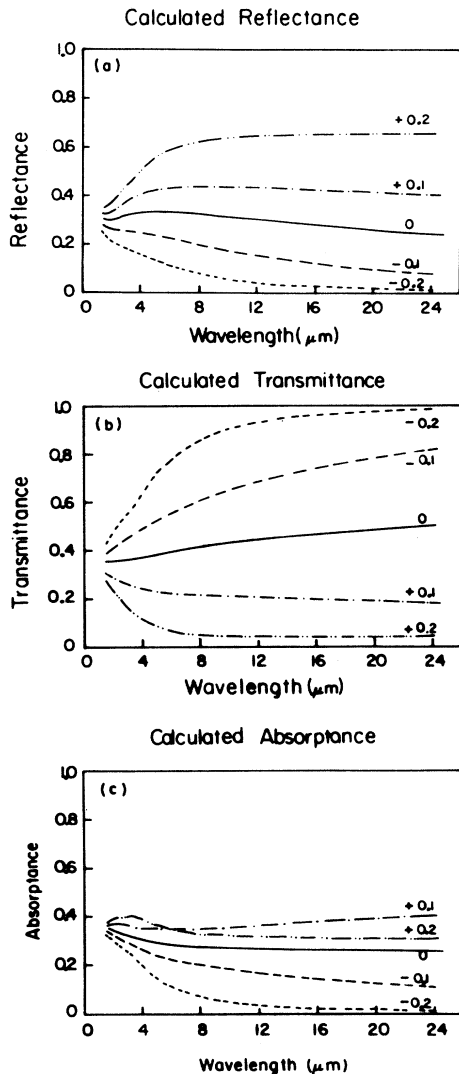


FIG. 7. Long-wavelength behavior of semicontinuous Au films for several values of the coverage parameter  $\delta p$  as indicated on the graphs. (a) Reflectance. (b) Transmittance. (c) Absorptance.

tribution from regions of zero dc-conductivity. The capacitance between adjacent clusters is very important in producing the optical response.

(5) The optical properties of the whole film are calculated by summing over the local contributions of small regions of linear size  $L(\omega)$ . The average ac conductivity does not reproduce the optical response correctly.

Optical measurements provide remarkable information about the microgeometry of semicontinuous metal films. A careful study of both the optical and the electrical properties of such films can be very useful for measuring, experimentally, such fundamental properties as critical exponents, scaling relations, and distribution functions. In addition, the crossover between different asymptotic behaviors can be studied. For example, the optical absorption in the range  $L(\omega) \approx \xi$  is sensitive to the exact form of the scaling function.

Optical measurements can also serve as a nondestructive method for examining the degree of homogeneity of thin films. As discussed in the previous section, small cracks and voids introduce extra capacitance which enhances the optical absorption. Again, microgeometrical details on length scales much shorter than the optical wavelength can be perceived in such measurements. We have shown that it is the *fluctuations* in the local conductivity that are crucial for determining the optical properties of a percolating medium. This work also includes an attempt to include capacitance effects as well as anomalous diffusion in the calculation of ac electrical properties of a percolating system.

We conclude by emphasizing the importance of microgeometrical effects in determining the optical response of semicontinuous metal films, and the remarkable amount of information obtainable from optical measurements. Measurements of semicontinuous metal films at longer wavelengths are needed to observe the crossover from inhomogeneous to homogeneous behavior.

#### ACKNOWLEDGMENTS

This research was supported in part by the C.N.R.S., by a grant from the US-Israel Binational Science Foundation, and by the Oren Family Foundation.

\*Present address: Cavendish Laboratory, Madingley Road, Cambridge CB3 0HE, UK.

<sup>1</sup>R. W. Cohen, G. D. Cody, M. D. Coutts, and B. Abeles, *Phys. Rev. B* **8**, 3689 (1973); P. Sheng, *Phys. Rev. Lett.* **45**, 60 (1980).

<sup>2</sup>S. Norrman, T. Andersson, C. G. Granqvist, and O. Hunderi, *Phys. Rev. B* **18**, 674 (1978).

<sup>3</sup>P. Gadenne, *Thin Solid Films* **57**, 77 (1979).

<sup>4</sup>S. Berthier, J. Lafait, C. Sella, and Thran-Khanh-Vien, *Thin Solid Films* **125**, 171 (1985).

<sup>5</sup>Y. Yagil and G. Deutscher, *Thin Solid Films* **152**, 465 (1987).

<sup>6</sup>P. Gadenne, A. Beghdadi, and J. Lafait, *Opt. Commun.* **65**, 17 (1988).

<sup>7</sup>P. Gadenne, these d'etat, Universite' de Paris VII (1986).

<sup>8</sup>M. Kunz, G. A. Niklasson, and C. G. Granqvist, *J. Appl. Phys.* **64**, 3740 (1988).

<sup>9</sup>K. A. Khan, G. A. Niklasson, and C. G. Granqvist, *J. Appl. Phys.* **64**, 3327 (1988).

<sup>10</sup>P. Gadenne, Y. Yagil, and G. Deutscher, *J. Appl. Phys.* **66**, 3019 (1989).

<sup>11</sup>J. C. Maxwell Garnett, *Philos. Trans. R. Soc. London* **203**, 385 (1904).

<sup>12</sup>D. Bruggemann, *Ann. Phys. (Leipzig) [Folge 5]* **24**, 636 (1935).

<sup>13</sup>Y. Yagil and G. Deutscher, *Appl. Phys. Lett.* **52**, 373 (1988).

<sup>14</sup>T. Robin and B. Souillard, in *Proceedings of 2nd International Conference on Electrical Transport and Optical Properties of Inhomogeneous Media, Paris, 1988*, edited by J. Lafait and D. B. Tanner (North-Holland, Amsterdam, 1989); *Physica A*

- 157, 285 (1989).
- <sup>15</sup>D. J. Bergman, Phys. Rev. B **19**, 2359 (1979).
- <sup>16</sup>D. J. Bergman, J. Phys. C **12**, 4947 (1979).
- <sup>17</sup>Y. Kantor and D. J. Bergman, J. Phys. C **15**, 2033 (1982).
- <sup>18</sup>B. Bedeaux and J. Vlieger, Thin Solid Films **102**, 265 (1983).
- <sup>19</sup>P. A. Bobbert and J. Vlieger, Physica A **147**, 115 (1987).
- <sup>20</sup>See, for instance, M. Born and E. Wolf, *Principles of Optics* (Pergamon, New York, 1975), 5th ed., p. 325.
- <sup>21</sup>A. P. Young and R. B. Stinchcombe, J. Phys. C **8**, L535 (1975).
- <sup>22</sup>A. L. Efros and B. I. Shklovskii, Phys. Status Solidi B **76**, 475 (1976).
- <sup>23</sup>R. B. Stinchcombe and B. P. Watson, J. Phys. C **9**, 3221 (1976).
- <sup>24</sup>S. Kirkpatrick, Phys. Rev. B **15**, 1533 (1977).
- <sup>25</sup>D. J. Bergman and Y. Imry, Phys. Rev. Lett. **39**, 1222 (1977).
- <sup>26</sup>J. P. Straley, Phys. Rev. B **15**, 5733 (1977).
- <sup>27</sup>R. Rosman and B. Shapiro, Phys. Rev. B **16**, 5117 (1977).
- <sup>28</sup>M. J. Stephen, Phys. Rev. B **17**, 4444 (1978).
- <sup>29</sup>R. Fisch and A. B. Harris, Phys. Rev. B **18**, 416 (1978).
- <sup>30</sup>B. Derrida, D. Stauffer, H. J. Herrmann, and J. Vannimenus, J. Phys. Lett. **44**, L701 (1983).
- <sup>31</sup>J. G. Zabolitzky, Phys. Rev. B **30**, 4077 (1984).
- <sup>32</sup>H. J. Herrmann, B. Derrida, and J. Vannimenus, Phys. Rev. B **30**, 4080 (1984).
- <sup>33</sup>C. J. Lobb and D. J. Frank, Phys. Rev. B **30**, 4090 (1984).
- <sup>34</sup>A. B. Harris and T. C. Lubensky, Phys. Rev. B **35**, 6964 (1987).
- <sup>35</sup>T. C. Lubensky and A. B. Harris, Phys. Rev. B **35**, 6987 (1987).
- <sup>36</sup>D. J. Frank and C. J. Lobb, Phys. Rev. B **37**, 302 (1988).
- <sup>37</sup>J. Adler, Y. Meir, A. Aharony, A. B. Harris, and L. Klein, J. Stat. Phys. (to be published).
- <sup>38</sup>Y. Gefen, A. Aharony, and S. Alexander, Phys. Rev. Lett. **50**, 77 (1983).
- <sup>39</sup>J. P. Straley, J. Phys. C **9**, 783 (1976).
- <sup>40</sup>J. P. Straley, J. Phys. C **13**, 819 (1980).
- <sup>41</sup>H. E. Stanley, P. J. Reynolds, S. Redner, and F. Family, in *Real Space Renormalization*, edited by T. W. Burkhardt and J. M. J. Van Leeuwen (Springer, Berlin, 1982).
- <sup>42</sup>R. Rammal, M. A. Lemieux, and A. M. S. Tremblay, Phys. Rev. Lett. **54**, 1087 (1985).
- <sup>43</sup>J. P. Straley, J. Phys. C **12**, 3711 (1979).
- <sup>44</sup>M. L. Theye, Phys. Rev. B **2**, 3060 (1970).
- <sup>45</sup>B. I. Halperin, S. Feng, and P. N. Sen, Phys. Rev. Lett. **54**, 2391 (1985).